

High temperature corrosion of silicon nitride composite ceramics in sulfur-oxygen environments^①

WANG Xin(王昕)^{1,2}, SUN Kang-ning(孙康宁)^{1,2}, LI Jing(李静)²,

YU Xue-gang(于薛刚)², YIN Yan-sheng(尹衍升)^{1,2}, YANG Lian-xi(杨连喜)

(1. Key Laboratory of Liquid Structure and Heredity of Materials, Ministry of Education, Shandong University, Jinan 250061, China;

2. Key Laboratory of Engineering Ceramics, Shandong Province, Shandong University, Jinan 250061, China)

Abstract: High temperature corrosion behavior of Si_3N_4 -8% Al_2O_3 (volume fraction) composite ceramics in sulfur-oxygen environments was studied. At 1150 °C and 1350 °C, the corrosion processes follow parabolic law with parabolic rate constants (K_p) of $1.45 \times 10^{-9} \text{ g}^2 \cdot \text{cm}^{-4} \cdot \text{s}^{-1}$ and $7.92 \times 10^{-9} \text{ g}^2 \cdot \text{cm}^{-4} \cdot \text{s}^{-1}$, respectively. The corrosion mechanisms are different at different temperatures. At 1150 °C, the corrosion of the material is due to the destruction of SiO_2 layer caused by sulfur and the active oxidation corrosion. At 1350 °C, the diffusion of additives and impurity elements to grain boundaries and outward to surface layers lead to the formation, growth and break of bubbles, which accelerates the corrosion rate of the Si_3N_4 ceramics.

Key words: Si_3N_4 composite ceramics; sulfidation; oxidation; corrosion

CLC number: TQ 126

Document code: A

1 INTRODUCTION

Si_3N_4 composite ceramics would be taken as a candidate materials for high temperature resistant parts in mineral fuel converting systems, such as coal-gasification, coal-fired power generation and industrial waste incineration, because of its excellent oxidation resistance and high temperature strength^[1]. In these systems, the combustion gas mixture of sulfur and oxygen is the main corrosive medium.

Up to now, the study on high-temperature corrosion of Si_3N_4 matrix ceramics was mainly concentrated on its oxidation behavior^[2-8]. There are few reports on the study of high-temperature sulfidation and the effects of high-temperature sulfur-oxygen atmosphere. This paper aims to investigate the high-temperature corrosion behavior of Si_3N_4 -8% Al_2O_3 ceramics in sulfur-oxygen environments.

2 EXPERIMENTAL

The raw materials were purchased Si_3N_4 powders (chemically pure, mean particle diameter is 2.5 μm), Al_2O_3 powder (chemically pure, mean particle diameter is 0.37 μm) and Y_2O_3 powder (chemically pure, mean particle diameter is 3.0 μm). Si_3N_4 -8% Al_2O_3 mixed powders were prepared by the multiphase suspension method^[9]. 0.5% Y_2O_3 (mass fraction) was added to

improve sintering properties. Ceramic blocks were obtained by hot-pressing sintering (35 MPa, 1650 °C for 1 h) in Multir-5000 functional furnace (Japan) and made into specimens of 10 mm × 10 mm × 3 mm. The samples with relative density of 98.6%, were polished and washed by ultrasonic cleaning in acetone for 30 min, then dried and heated (30 °C/min) to 1150 °C or 1350 °C in self-made vacuum pipe furnace. H_2S and O_2 were aerated into the pipe. The flow velocity and pressure of gases could be controlled by the pressure gauges. The environment atmosphere of specimens was kept as: at 1150 °C, $p(\text{O}_2) = 1.8 \times 10^{-2} \text{ Pa}$, $p(\text{H}_2\text{S}) = 44 \text{ Pa}$; at 1350 °C, $p(\text{O}_2) = 1.4 \times 10^{-2} \text{ Pa}$, $p(\text{H}_2\text{S}) = 320 \text{ Pa}$. Gas feeding continued until the temperature dropped to 600 °C. Corroded specimens were weighed following their removal from the relevant environment and corrosion extents were expressed as mass gain. The corrosive surface of specimens was observed by scanning electron microscope (JAX-840).

3 RESULTS

3.1 Corrosion kinetics curves

Figs. 1 and 2 show the corrosion kinetics curves of Si_3N_4 ceramics in oxygen-sulfur environments at different temperatures (i. e. the relationship between mass gain of specimen and corrosion time). It is obvi-

① Foundation item: Project (Y2001F01) supported by the Natural Science Foundation of Shandong Province, China

Received date: 2002-04-27; Accepted date: 2002-07-05

Correspondence: Prof. WANG Xin, Tel: +86-531-8392439; E-mail: wang-xin@163.com

ous that at 1 150 °C the corrosion process of the ceramics almost follows the parabolic law of diffusion reaction kinetics with a parabolic rate constant:

$$K_p = 1.45 \times 10^{-9} \text{ g}^2 \cdot \text{cm}^{-4} \cdot \text{s}^{-1}$$

While at 1 350 °C, the corrosion kinetics curve of Si_3N_4 ceramics deviates from the parabolic law instead, the corrosion rate decreases with corrosion time after an early increasing period of about 24 h.

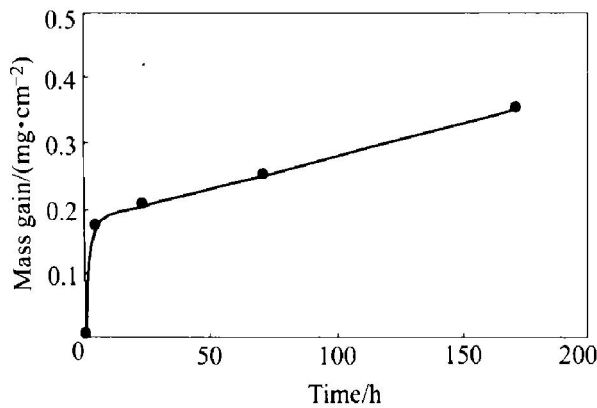


Fig. 1 Mass gain of samples vs time in sulfur-oxygen environments at 1 150 °C

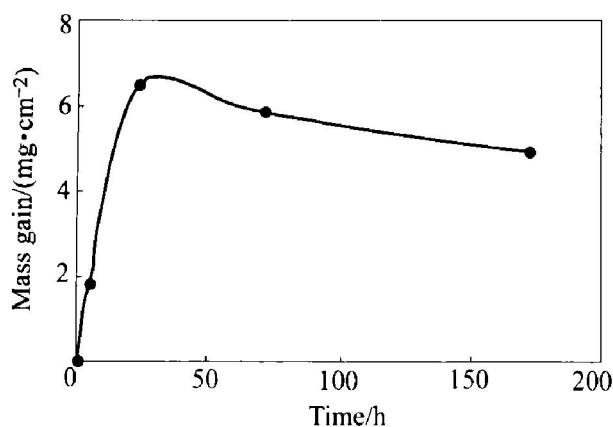


Fig. 2 Mass gain of samples vs time in sulfur-oxygen environments at 1 350 °C

3.2 SEM results

Figs. 3 and 4 are SEM morphologies of corrosion surface of the samples at 1 350 °C and 1 150 °C, respectively. The former shows that lots of bubbles formed on the surface of the ceramics corroded at 1 350 °C for 24 h and the bubbles have not broken yet (Fig. 3(a)). After 72 h, not only the diameter of bubbles increased greatly, but also most of them broke (Fig. 3(b)). At 1 150 °C, there was no sign of bubble formation on sample surface even for 72 h corrosion, but white dots of oxide formed and grew on the surface (Fig. 4).

Fig. 5 shows SEM micrographs of cross-sectional surface of samples at 1350 °C, which can more clearly reflect the formation and break of the

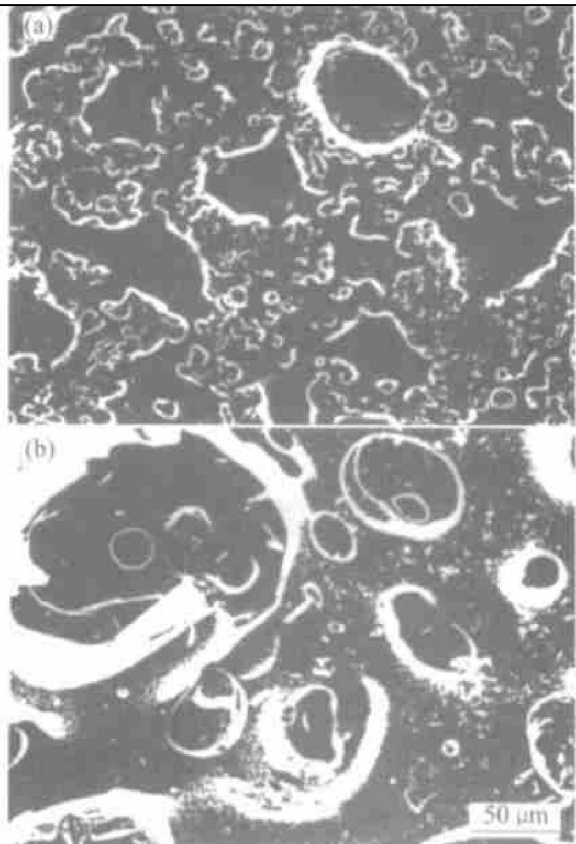


Fig. 3 SEM micrographs of sample surface corroded at 1 350 °C for different time
(a) 24 h; (b) 72 h

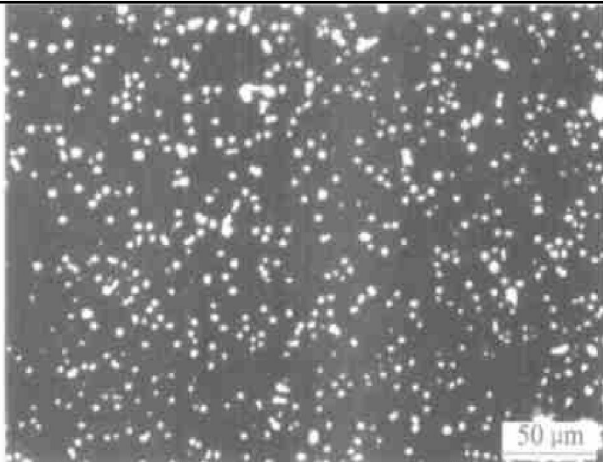


Fig. 4 SEM micrographs of sample surface corroded at 1 150 °C for 72 h

bubbles on the sample surface. After 5 h corrosion, the surface of corrosion layer is relatively smooth and bubbles are forming and growing (Fig. 5(a)). 72 h later, the thickness of corrosion layer increased greatly. The concave-convex surface of samples was created by the break down a great quantity of bubbles that also led to some bubbles connecting together, which provided channels for corrosion to develop into the inner part of the samples (Fig. 5(b)).

3.3 Microstructure analysis

Fig. 6 shows that some elements such as Y, Al, O

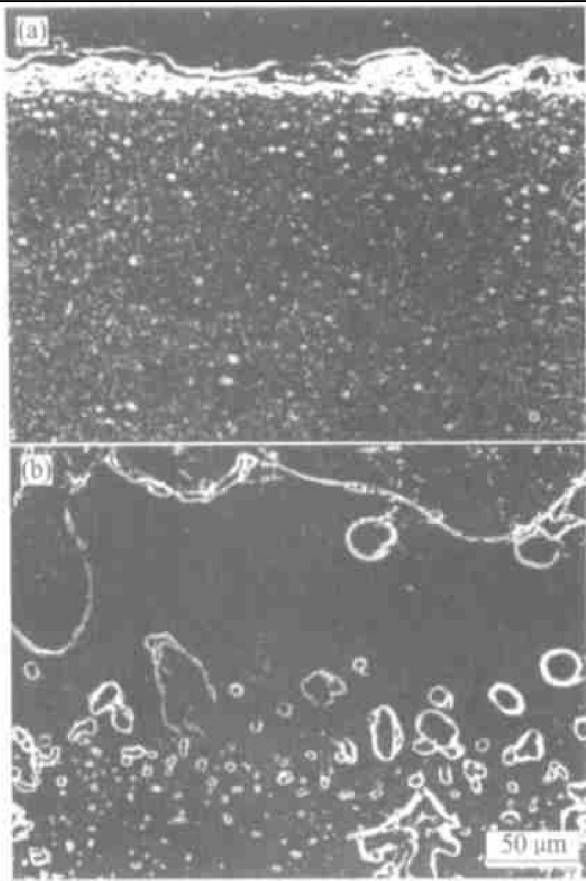


Fig. 5 SEM micrographs of cross-sectional surface of samples corroded at 1350 °C for different time
(a) 5 h; (b) 72 h

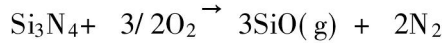
were abundant in the outer layer of the samples. It would be noted that sulfur appeared also, suggesting that sulfur played a role in the processes of formation and growth of bubbles, and sulfur went into the bubbles in some forms (SiS)^[10]. Although at high temperature SiS exists in the form of gas, maybe it can not escape and exists inside the bubbles even going into the surface layer of the

samples after cooling down.

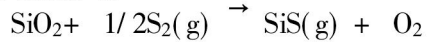
4 DISCUSSION

In oxidation atmosphere, SiO_2 layer formed a corrosion barrier through reaction of Si_3N_4 with oxygen and the further oxidation occurs only by the inward diffusion of oxygen through silica layer. So the corrosion rate is low. Its parabolic rate constant at 150 °C is about^[5] $1.0 \times 10^{-13} \text{ g}^2 \cdot \text{cm}^{-4} \cdot \text{s}^{-1}$.

In our experiment of corrosion in sulfur-oxygen atmosphere, the parabolic rate constant is nearly 10^4 times larger than that in pure oxygen at the same temperature. This means the corrosion mechanism here is different from oxidation. While the partial pressure of sulfur is much higher than oxygen in the corrosion atmosphere of our experiment, it is possible that the following reaction may occur preferentially^[6, 11, 12]:



It is called active oxidation. On the other hand, even though silicon reacts with oxygen to form SiO_2 in priority, the SiO_2 formed may continue to react with sulfur as



The volatile SiS can destroy oxide films so as to increase the corrosion rate. Therefore, the corrosion rate of Si_3N_4 matrix ceramics in sulfur-oxygen mixed gases is far greater than in oxygen. At 1350 °C, the corrosion kinetics curve (Fig. 2) doesn't follow parabolic law. It may be due to that Si_3N_4 ceramics could react with O_2 and produce N_2 bubbles, and the protection of oxide films could be destroyed because of break of these bubbles and the escaping of volatile corrosion products. But if the corrosion kinetics is expressed by virtue of the variation of thickness of material loss with exposure time, the corrosion

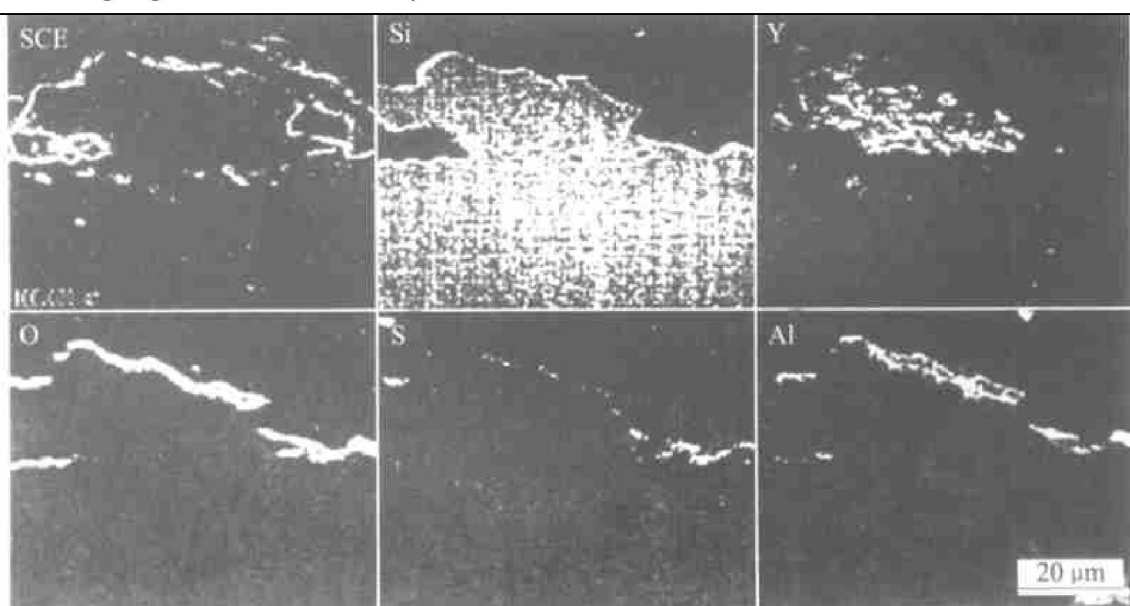


Fig. 6 SEM micrograph of cross-sectional surface of samples corroded at 1350 °C for 5 h as well as distribution of elements Si, Y, O, S and Al

process still follows the parabolic law. Fig. 7 shows the relationship of thickness of material loss and exposure time at 1 350 °C in oxygen-sulfur. The parabolic rate constant is

$$K'_p = 2.1 \times 10^{-13} \text{ m}^2 \cdot \text{s}^{-1}$$

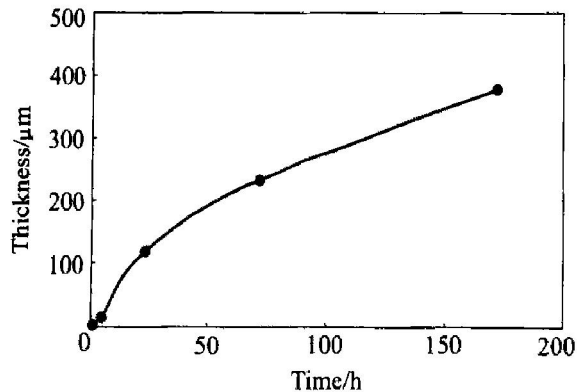


Fig. 7 Relationship of thickness of material loss vs exposure time at 1 350 °C

According to Ref. [7], $1 \text{ m}^2 \cdot \text{s}^{-1}$ can be converted to $3.77 \times 10^6 \text{ kg}^2 \cdot \text{cm}^{-4} \cdot \text{s}^{-1}$. So the parabolic rate constant above could be expressed as follows with corrosion mass gain as a factor instead of corrosion thickness:

$$K_p = 7.92 \times 10^{-9} \text{ g}^2 \cdot \text{cm}^{-4} \cdot \text{s}^{-1}$$

which is 4~5 times higher than that at 1 150 °C. The reason why the corrosion rate increases greatly is that the diffusion activity of additives (Al, Y) and impurity elements increases with increasing temperature, which leads to the enrichment of these elements in the surface and grain boundaries to form Y_2O_3 - Al_2O_3 - SiO_2 eutectic phases with low melting point. Therefore, bubbles could easily form, grow and break in these areas, which provides channels for corrosive gases to penetrate onto the samples. It can be concluded that at 1 350 °C the corrosion arises due to common effects of corrosive gases diffusing inward and impurity elements diffusing outward. Because the diffusion rate of corrosive gases is higher, the diffusion of impurities becomes the dominant factor during the corrosion process.

5 CONCLUSIONS

1) The corrosive kinetics follow parabolic law at 1 150 °C and 1 350 °C with parabolic rate constants at 1 150 °C, $K_p = 1.45 \times 10^{-9} \text{ g}^2 \cdot \text{cm}^{-4} \cdot \text{s}^{-1}$; at 1 350 °C, $K_p = 7.92 \times 10^{-9} \text{ g}^2 \cdot \text{cm}^{-4} \cdot \text{s}^{-1}$

2) At 1 150 °C, the active oxidation under

lower oxygen partial pressure and the destruction of SiO_2 protection layer caused by sulfur are the main reasons to the corrosion of Si_3N_4 matrix ceramics.

3) At 1 350 °C, the main factor affecting the corrosion of Si_3N_4 -matrix ceramics in oxygen-sulfur environments is the diffusion of additives and impurities to grain boundaries and surface layers, which results in the formation of some eutectic phases with low melting points so that the corrosion rate increases because liquid eutectic phases facilitate the formation, growth and break of bubbles on the sample surface.

REFERENCES

- [1] Jacobson N S. Corrosion of silicon ceramics in combustion environments [J]. *J Am Ceram Soc*, 1993, 76(1): 3~28.
- [2] Hirai T, Niihara K, Goto T. Oxidation of CVD Si_3N_4 at 1 550 °C to 1 650 °C [J]. *J Am Ceram Soc*, 1980, 63(7): 419~424.
- [3] Du H, Treasslar R E, Pantano C G. Oxidation of studies of crystalline CVD silicon nitride [J]. *J Electrochem Soc*, 1989, 136(5): 1527~1536.
- [4] Lin S. Mass spectrometric analysis of the vapor in oxidation of Si_3N_4 compacts [J]. *J Am Ceram Soc*, 1975, 58(3~4): 160~165.
- [5] Schlichting J, Gauckler L J. Oxidation of some β - Si_3N_4 Materials [J]. *Powder Metall Int*, 1977, 9(1): 36~39.
- [6] Huer A H. Volatility diagram for silicon, silicon nitride and silicon carbide and application to high-temperature decomposition and oxidation [J]. *J Am Ceram Soc*, 1990, 73(10): 2798~2803.
- [7] Lutha K L. Some new perspectives on oxidation of silicon carbide and silicon nitride [J]. *J Am Ceram Soc*, 1989, 69(5): 1095~1103.
- [8] YANG Haifeng, TANG Yuling. Densification and phase transformation during sintering of Si_3N_4 ceramics [J]. *Trans Nonferrous Met Soc China*, 1996, 6(4): 150~153.
- [9] WANG Xin, TAN Xuruiyan, YIN Yansheng. Preparation of nano ceramic composites by mixing multi-phases aqueous suspensions [J]. *J Ceramics*, 1999, 20(1): 5~8. (in Chinese)
- [10] LIANG Yingjiao. *Handbook of Thermodynamics Data of Inorganic Compounds* [M]. Shenyang: Northeastern University Press, 1993. 473. (in Chinese)
- [11] LUO Xuetao, YUAN Rurzhang. Effect of high-temperature oxidation and thermal shock on mechanical properties of Y-La-Si₃N₄ ceramics [J]. *J Wuhan Univ of Techno*, 1998, 20(1): 16~20. (in Chinese)
- [12] Singhal S C. Thermodynamics and kinetics of oxidation of hot-pressed Si_3N_4 [J]. *J Mater Sci*, 1976, 11(3): 500~506.

(Edited by LONG Huai-zhong)